IEEE Photonics Journal
An IEEE Photonics Society Publication

Open Access

Noise Investigation of a Large Free Spectral Range High-Resolution Microwave Photonic Signal Processor

Volume 5, Number 6, December 2013

Erwin H. W. Chan

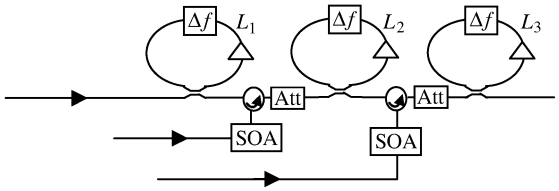

DOI: 10.1109/JPHOT.2013.2289959
1943-0655

IEEE photonics SOCIETY

IEEE

Noise Investigation of a Large Free Spectral Range High-Resolution Microwave Photonic Signal Processor

Erwin H. W. Chan

School of Electrical and Information Engineering, Institute of Photonics and Optical Science, The University of Sydney, Sydney, N.S.W. 2006, Australia

DOI: 10.1109/JPHOT.2013.2289959

Manuscript received July 16, 2013; revised October 28, 2013; accepted October 29, 2013. Date of publication November 7, 2013; date of current version November 20, 2013. This work was supported by the Australian Research Council. Corresponding author: E. H. W. Chan (e-mail: erwin.chan@sydney.edu.au).

Abstract: The noise components in a new microwave photonic signal processor that has the ability of simultaneously realizing a large free spectral range (FSR) and high-resolution bandpass filter response are investigated. The filter is implemented using the Vernier effect and the frequency-shifting technique in an optical delay line structure. The power spectrum of the signal-spontaneous beat noise, which is the dominant noise source in the system, is theoretically analyzed and experimentally measured. Experimental results are presented, which show that the new large FSR microwave photonic signal processor has a low-noise performance and demonstrate 31-fold increase in the FSR of a bandpass filter response while having a sharp passband and 30-dB stopband rejection level.

Index Terms: Fiber optics systems, electrooptical systems, coherent effects.

1. Introduction

Photonic signal processing is attractive due to its high time-bandwidth capability, immunity to electromagnetic interference, and its potential to solve the limitations of electronic approaches. It can also process signals directly inside the fiber [1]. Photonic signal processors implemented using the infinite impulse response (IIR) optical delay line structures such as the amplified recirculating delay line (ARDL) loop [2] and the active-fibre Bragg-grating-pair cavity [3] can generate a large number of delayed optical signals to realize a high-resolution bandpass filter response, using only few optical components. However, these filters have a limited operating bandwidth because they have a periodic frequency response where the filter passband repeats at an integer multiple of the fundamental filter passband frequency. The separation between two successive passbands of the filter is referred to as the free spectral range (FSR) [4]. A large FSR is required for a filter to operate over a wide bandwidth.

The filter FSR is determined by the time delay of the delayed optical signals, which in turn depends on the loop length of an IIR optical delay line structure. A large-FSR bandpass filter requires the IIR optical delay line structure to have a short loop length. The loop length of an IIR optical delay line structure is restricted by the components inside the delay line loop. An optical amplifier is required inside the delay line loop to compensate for the loop loss and to provide gain for generating a large number of delayed optical signals so that a high-resolution bandpass filter response can be obtained. A passive recirculating delay line with a short loop length of 2.8 cm has been fabricated on a lithium niobate waveguide [5]. With the inclusion of a few centimeter long

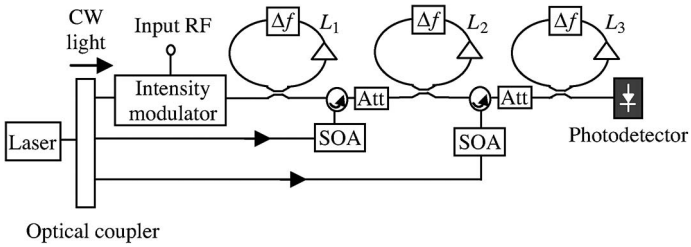

Fig. 1. Topology of the large-FSR high-resolution microwave photonic bandpass filter.

erbium-doped waveguide amplifier [6], the length of the integrated ARDL loop can be 10 cm. This shows an IIR-based optical delay line signal processor can only realize a bandpass filter response with a maximum FSR of around 1.4 GHz even the device is integrated in a lithium niobate waveguide that has 2.14 refractive index. This makes the filter operating bandwidth to be less than 2.8 GHz, which is too low for many applications.

Recently, Vernier effect [7] has been used in microwave photonic signal processing to increase the filter frequency response FSR [4], [8]–[10]. These filters are based on connecting two optical delay line structures in series with proper design on the delay time of each structure. While these structures have demonstrated the increase in the frequency response FSR, they either have limited resolution or generate an excessive amount of phase-induced intensity noise (PIIN) which limits the signal-to-noise ratio (SNR) [11] that makes them unusable in practice. Recently, we reported a technique, based on the use of a time compression unit, to increase the FSR of a microwave photonic bandpass filter [12]. This filter has no PIIN but only a low-resolution filter response was demonstrated. The aim of this paper is to present for the first time that the theoretical and experimental investigation of the noise presented in a new large-FSR high-resolution microwave photonic bandpass filter implemented using the Vernier effect. The filter features the advantages of PIIN-free and robust performance. Experimental results are presented that demonstrate a high-resolution bandpass filter with 31-fold increase in the frequency response FSR. The filter SNR performance are also measured and compared with a simple optical delay line structure.

2. Filter Topology

Fig. 1 shows the topology of the new large-FSR high-resolution microwave photonic bandpass filter. The continuous wave (CW) light from a laser source is split by an optical coupler. The light at the first coupler output is intensity modulated by an optical modulator driven by an RF signal. The RF modulated optical signal at the modulator output circulates in the first frequency shifting amplified recirculating delay line (FS-ARDL) loop with a loop length L_1. This generates many different frequency delayed optical signals, which produce a coherence-free high-resolution bandpass filter response [13]. The delayed optical signals together with the CW light from one of the optical coupler outputs are launched into a wavelength converter formed by an optical circulator and a semiconductor optical amplifier (SOA). The function of the wavelength converter is to copy the processed RF information signal carried by the different frequency delayed optical signals into the CW light through the process of cross gain modulation (XGM) in the SOA [14]. The single frequency optical signal at the output of the wavelength converter has a coherence-free high-resolution bandpass filter response. It passes through an optical attenuator (Att) before launching into the second FS-ARDL loop with a loop length L_2. The optical attenuator is used to control the signal power into the second loop to avoid saturating the optical amplifier inside the second loop. The RF information signal at the second FS-ARDL output, which has been processed twice, is again copied to the CW light from one of the optical coupler outputs via the XGM effect in the SOA. The single frequency optical signal carrying the processed RF information signal launches into the third FS-ARDL with a loop length L_3 for signal processing for the third time, and is then detected by the photodetector.

According to the Vernier effect, the transfer function of the structure shown in Fig. 1 is the product of the transfer function of each FS-ARDL loop. The FSR of the overall structure is the least common

multiple of the FSR of each FS-ARDL loop [7], which is given by

$$FSR = k_1 FSR_1 = k_2 FSR_2 = k_3 FSR_3 \tag{1}$$

where k_m is an integer and FSR_m is the FSR of the frequency response produced by the mth FS-ARDL loop, which is given by

$$FSR_m = \frac{c}{nL_m} \tag{2}$$

where c is the speed of light, n is the fiber refractive index and L_m is the loop length of the mth FS-ARDL. Therefore, in order to obtain a large increase in the FSR, the loop length of the FS-ARDLs shown in Fig. 1 need to be designed so that they are not an integer multiple of the others.

The frequency shift Δf in each loop shown in Fig. 1 can be the same or different to that in the other loops. It only needs to be three times larger than the maximum RF signal frequency in order to avoid the aliasing problem [1]. Since the delayed optical signals into the wavelength converters and into the photodetector have different optical frequencies (or wavelengths), the structure shown in Fig. 1 has no coherent interference and PIIN problems. Hence, a robust bandpass filter response can be obtained.

It should be pointed out that a microwave photonic bandpass filter implemented using multiple ARDL loops has been reported [15]. However, the previously reported structure is not aimed to increase the frequency response FSR and to obtain a low-noise performance. It is aimed to improve the filter response skirt selectivity by designing all the ARDL loops to have the same length so that the filter passbands generated by the loops are aligned with each other. This is different to the large-FSR microwave photonic bandpass filter presented in this paper where the loops are designed to have different lengths, and consist of an optical frequency shifter for PIIN suppression. Moreover, until now there have been no reports on the investigation of the noise components generated by a multiple coherence-free optical delay line structure.

3. Filter Transfer Function and Noise Analysis

The large-FSR high-resolution microwave photonic bandpass filter transfer function, which is defined as the ratio of the output and input RF signal voltage, is given by

$$H(f) = \prod_{m=1}^{M} \left[(1 - \kappa_m) + \kappa_m^2 \sum_{i=1}^{N_m} g_m^i l_m^i (1 - \kappa_m)^{i-1} z_m^{-i} \right] \cdot \prod_{m=1}^{M-1} [\eta_m(f) G_m Att_m] \tag{3}$$

where $M > 1$ is the number of the FS-ARDL loops, N_m is the number of taps generated in the mth loop, κ_m is the coupling ratio of the optical coupler in the mth loop, g_m is the gain of the optical amplifier inside the m th loop, l_m is the insertion loss of the optical frequency shifter inside the mth loop, $z_m = \exp(j2\pi T_m f)$, f is the RF frequency, $T_m = (nL_m)/c$ is the delay time corresponding to the mth FS-ARDL loop length L_m, $\eta_m(f)$ is the XGM wavelength conversion efficiency of the mth wavelength converter, G_m is the ratio of the optical power at the output and input of the mth wavelength converter, and Att_m is the attenuation of the mth optical attenuator. The first term in (3) is the product of the M FS-ARDL loop transfer functions. The second term is due to the XGM effect in the SOAs. Since SOAs can be designed to have a wide XGM bandwidth [14], the XGM wavelength conversion efficiency response is flat for the frequencies below 40 GHz. Therefore, the overall filter response shape is simply determined by the frequency responses of the M FS-ARDL loops, which can be controlled by the system parameters such as the optical coupler coupling ratios, the optical amplifier gains and the loop lengths.

As an example, we consider the design of a high-resolution microwave photonic bandpass filter that has a fundamental passband frequency at 4.275 GHz, a 500 kHz 3-dB passband width and an over 30 dB stopband rejection level. This cannot be realized by using the single-loop structure because the loop length of the FS-ARDL needs to be 3.3 cm, which is too short even the device is integrated in a lithium niobate waveguide. However, the dual-loop structure can be used to satisfy

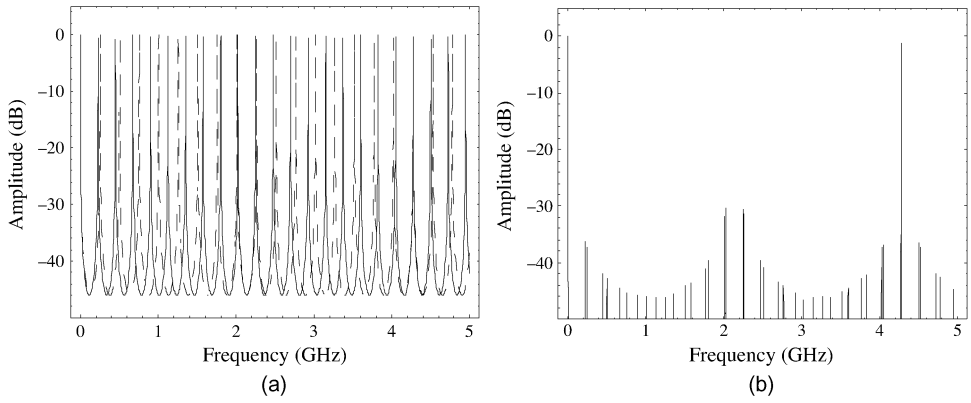

Fig. 2. (a) Frequency responses of the first (solid) and second (dash) FS-ARDL microwave photonic bandpass filters with the loop lengths of 62.3 cm and 55.7 cm, respectively. The filter 3-dB passband widths are around 1.1 MHz. (b) Frequency response of the dual FS-ARDL large-FSR microwave photonic bandpass filter. The filter 3-dB passband width is 500 kHz.

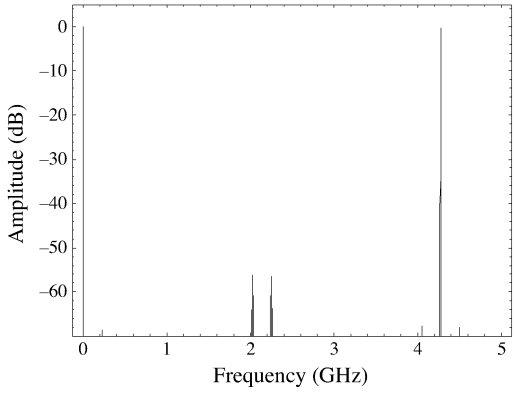

Fig. 3. Frequency response of the triple FS-ARDL large-FSR microwave photonic bandpass filter. The filter 3-dB passband width is 500 kHz.

the design requirements. The first FS-ARDL loop length is designed to be 62.3 cm, which corresponds to an FSR of 225 MHz and is 19 times less than the designed filter FSR. The second FS-ARDL loop length is designed to be 55.7 cm, which corresponds to an FSR of 251.47 MHz and is 17 times less than the designed filter FSR. The two FS-ARDL loops have the same loop gain of $\kappa gl = 0.99$. The frequency responses of the two FS-ARDL loops and the combined response are shown in Fig. 2. This shows a 17-fold increase in the filter frequency response FSR can be achieved by using the dual-loop structure. The unwanted passbands are more than 30 dB below the wanted passband at 4.275 GHz. The filter 3-dB passband width is 500 kHz. Note that both the stopband rejection level and the 3-dB passband width of the dual-loop large-FSR microwave photonic bandpass filter are dependent on the loop gains of the FS-ARDLs. A higher stopband rejection level can be achieved by increasing the loop gain but this will alter the 3-dB passband width of the filter. By connecting another FS-ARDL loop after the dual-loop structure to form a triple FS-ARDL loop as shown in Fig. 1 can provide an extra degree of freedom in controlling the stopband rejection level and the 3-dB passband width of the filter. Fig. 3 shows the frequency response of the triple-loop structure having the loop lengths of 68.9 cm, 62.3 cm and 55.7 cm, and the same loop gain of 0.987 for the three loops. In this case, the filter 3-dB passband width remains 500 kHz while the filter stopband rejection level is increased to over 55 dB.

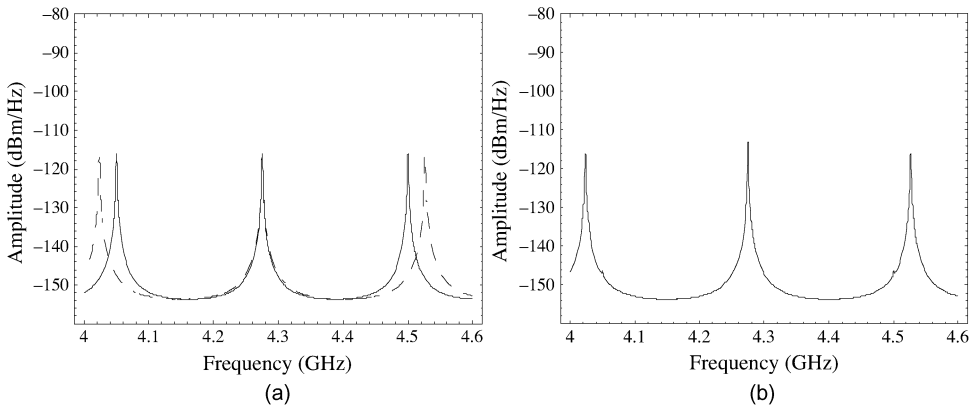

Fig. 4. (a) Simulated s-sp beat noise spectrums of the FS-ARDL microwave photonic bandpass filters with 225 MHz (solid) and 251.47 MHz (dash) FSR. (b) Simulated s-sp beat noise spectrum of the dual-loop large-FSR microwave photonic bandpass filter.

Since the PIIN generated in the FS-ARDL is frequency shifted to be outside the RF information band, the signal-spontaneous (s-sp) beat noise generated by the optical amplifier inside the FS-ARDL loop is the dominant noise source in the system. It was found that the s-sp beat noise generated in the FS-ARDL is 40 dB below the PIIN generated in the conventional ARDL [13]. Therefore, the FS-ARDL structure has the ability to realize a bandpass filter response with a low-noise performance. In the case of the dual FS-ARDL loop structure, the CW light into the wavelength converter copies both the processed RF information signal and the s-sp beat noise generated in the first loop to a single frequency optical signal that launches into the second loop. The second loop filters the noise generated in the first loop as well as generates its own noise [16]. Therefore, the s-sp beat noise spectrum at the output of the dual FS-ARDL large-FSR microwave photonic bandpass filter is given by

$$S_{s-sp}(f) = S_{s-sp,1}(f)\eta_1(f)G_1 Att_1|H_2(f)|^2 + S_{s-sp,2}(f) \tag{4}$$

where $S_{s-sp,m}(f)$ is the s-sp beat noise spectrum of the mth FS-ARDL [13], and $H_m(f)$ is the transfer function of the mth FS-ARDL and is given by

$$H_m(f) = (1-\kappa_m) + \kappa_m^2 \sum_{i=1}^{N_m} g_m^i l_m^i (1-\kappa_m)^{i-1} z_m^{-i}. \tag{5}$$

In the case of the large-FSR microwave photonic bandpass filter having M FS-ARDL loops, the power spectrum of the dominant s-sp beat noise is given by

$$S_{s-sp}(f) = \sum_{m=1}^{M-1}\left[S_{s-sp,m}(f)\prod_{n=m}^{M-1}\eta_n(f)G_n Att_n|H_{n+1}(f)|^2\right] + S_{s-sp,M}(f). \tag{6}$$

Fig. 4 shows the s-sp beat noise spectrums of two single FS-ARDL loop microwave photonic bandpass filters with the loop lengths of 62.3 cm and 55.7 cm, respectively, and the s-sp beat noise spectrum of the large-FSR microwave photonic bandpass filter formed by two FS-ARDL loops. The frequency responses of these filters are shown in Fig. 2. The fundamental passband frequency of the dual FS-ARDL loop microwave photonic bandpass filter is 4.275 GHz. In order to compare the s-sp beat noise level generated in the single and dual FS-ARDL loop structures, the optical attenuator attenuation in the dual-loop structure is set to be

$$Att_1 = \frac{1}{G_1 \cdot |H_1(0)|^2} \tag{7}$$

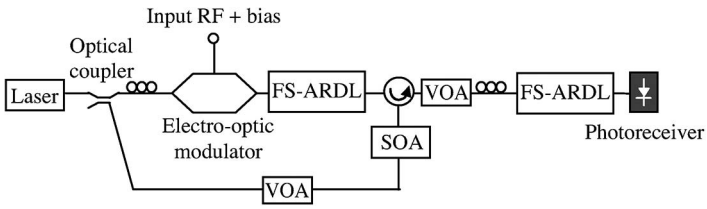

Fig. 5. Experimental setup of the large-FSR high-resolution microwave photonic bandpass filter.

so that the average output optical power of the dual-loop structure is the same as that of the single-loop structure. It can be seen from Fig. 4(b) that the s-sp beat noise peaks generated in the first loop at 4.05 GHz and 4.5 GHz are filtered by the second loop. The s-sp beat noise at the passband of the dual-loop large-FSR microwave photonic bandpass filter is 3 dB higher than that of the single FS-ARDL microwave photonic bandpass filter. Since the average output optical power into the photodetector is the same for both cases, the SNR of the dual-loop large-FSR microwave photonic bandpass filter is only 3 dB lower than that of the single FS-ARDL microwave photonic bandpass filter. Hence, the advantage of low-noise performance in the FS-ARDL remains in the dual-loop structure. Most importantly, the FSR of the frequency response generated by the dual-loop structure is significantly increased compared to the single-loop structure.

4. Experimental Results

An experiment was set up as shown in Fig. 5 to verify the concept of the large-FSR high-resolution microwave photonic bandpass filter. The optical source was a tunable external cavity laser. The laser wavelength was 1550 nm and the laser linewidth was less than 500 kHz. The CW light from the laser source was split by a 50 : 50 optical coupler. One of the optical coupler outputs was connected to a polarization controller followed by a quadrature biased electro-optic intensity modulator. The RF modulated optical signal at the modulator output was launched into an FS-ARDL, which was formed by a 50 : 50 optical coupler, an erbium-doped fibre amplifier (EDFA), an optical filter and a 250 MHz acousto-optic frequency shifter (AOFS). The delayed optical signals at the output of the FS-ARDL and the CW light from the laser source were fed into a wavelength converter, which comprised an optical circulator and a SOA. The variable optical attenuator (VOA) in front of the SOA was used to control the CW light power into the SOA to obtain a high XGM wavelength conversion efficiency. The output of the wavelength converter passed through a VOA before entering the second FS-ARDL. The second FS-ARDL was formed by the same components as in the first FS-ARDL except a 750 MHz AOFS was used instead of the 250 MHz AOFS. The 750 MHz AOFS had a 4 dB polarization dependence loss. Hence, polarization controllers at input of the second loop and inside the loop were used to ensure the recirculating optical signals were aligned to the frequency shifter input polarization. A variable optical delay line was inserted into the second FS-ARDL to adjust the loop length to increase the overall frequency response FSR. The delayed optical signals at the output of the second loop were detected by a photoreceiver, whose output was connected to a network analyzer to display the filter transfer characteristic. The loop lengths of the FS-ARDLs were obtained from the filter frequency response FSRs measured on the network analyzer with a 10 kHz resolution. By using (2) together with the measured FSRs, the loop lengths of the first and second FS-ARDLs were found to be 32.26 m and 24.78 m, respectively. Note that shorter loop lengths, which enable the filters to have larger FSRs, can be realized by using a linear SOA instead of an EDFA inside the loops. However, due to the lack of two linear SOAs, the large-FSR high-resolution microwave photonic bandpass filter was demonstrated using EDFAs.

Fig. 6 shows the measured and simulated frequency responses of the dual-loop large-FSR microwave photonic bandpass filter. Excellent agreement can be seen. The filter has a sharp 3-dB passband width of 15 kHz and over 30 dB stopband rejection level. The filter frequency response FSR was 80.7 MHz. A larger FSR can be obtained by adjusting the length of the second loop.

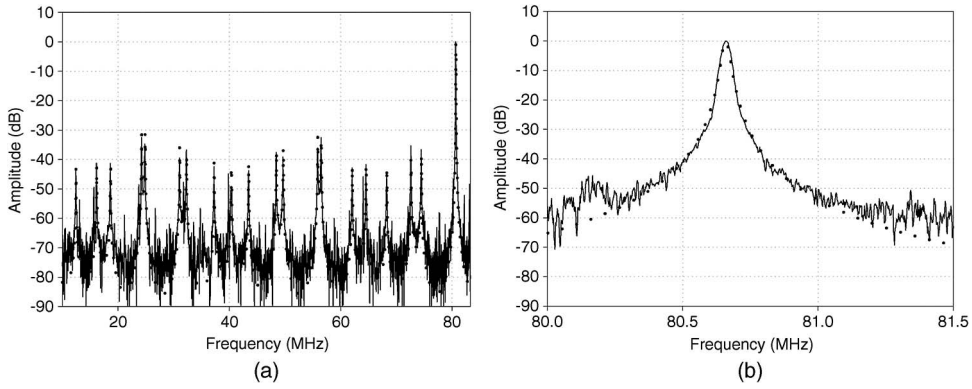

Fig. 6. Measured (solid) and simulated (dots) frequency responses of the dual-loop large-FSR microwave photonic bandpass filter. (a) Wideband response and (b) detailed section of the response within 1.5 MHz of the passband frequency.

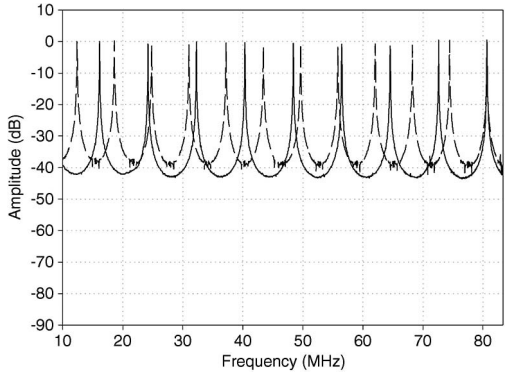

Fig. 7. Measured frequency responses of the single FS-ARDL microwave photonic bandpass filters with 6.2 MHz (dash) and 8.07 MHz (solid) FSR.

However, due to the aliasing problem, the maximum operating frequency of the FS-ARDL based microwave photonic bandpass filter was limited to one-third of the frequency shift, which was 83.3 MHz when using the 250 MHz AOFS. The filter frequency response was stable even the laser source had a narrow linewidth, which demonstrated the filter was free of coherent interference problem. The frequency responses of the first and second FS-ARDL loops were also measured and are shown in Fig. 7. The filter frequency response FSRs were 6.2 MHz and 8.07 MHz, respectively. This demonstrates 10-fold increase in the FSR can be achieved by using the dual FS-ARDL loop structure.

The SNRs of the single and dual FS-ARDL microwave photonic bandpass filters were measured by applying an RF signal at the filter passband frequency into the electro-optic intensity modulator. The output RF signal power and the output noise power were measured on an electrical spectrum analyzer connected to the photoreceiver. A low noise power was obtained at the output of the single and dual FS-ARDL microwave photonic bandpass filters demonstrating there was no PIIN. The measured single and dual FS-ARDL microwave photonic bandpass filter SNRs at the filter passband were 47.2 dB and 43.9 dB, respectively in a 100 kHz resolution bandwidth. This shows the SNR of the dual-loop structure is around 3 dB lower than that of the single-loop structure, which is agreed with the theoretical prediction. Although the dual FS-ARDL microwave photonic bandpass filter has a 3 dB lower SNR, it has a much larger frequency response FSR than the single FS-ARDL microwave photonic bandpass filter.

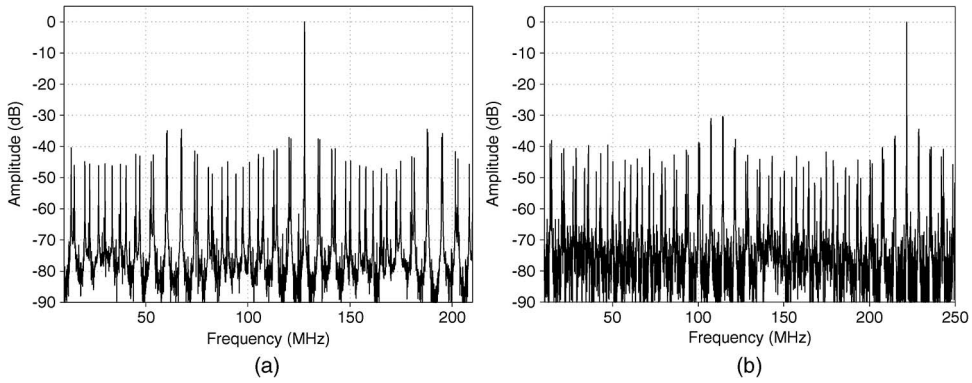

Fig. 8. Measured frequency responses of the dual-loop large-FSR microwave photonic bandpass filter for different second FS-ARDL loop lengths of (a) 26.592 m and (b) 27.917 m.

Finally, experiments were carried out to demonstrate a larger FSR bandpass filter response can be obtained by using the dual-loop structure. This was achieved by replacing the 250 MHz AOFS in the first FS-ARDL loop with a single-sideband suppressed carrier (SSB-SC) modulator based frequency shifter [17]. The SSB-SC modulator based frequency shifter can provide a larger frequency shift compared to the AOFS, which enables the filter to be demonstrated over a wider frequency range without the aliasing problem. The SSB-SC modulator was set up to provide a 2 GHz frequency shift. The length of the first FS-ARDL loop was 29.7 m, which resulted in a bandpass filter response with an FSR of 6.73 MHz. Fig. 8 shows the frequency responses of the dual-loop large-FSR microwave photonic bandpass filter for the second FS-ARDL having a loop length of 26.592 m $(\text{FSR} = 7.52\ \text{MHz})$ and 27.917 m $(\text{FSR} = 7.164\ \text{MHz})$, respectively. It can be seen from the figure that the combined response has a passband at 127.9 MHz and 222.1 MHz, which demonstrated 17-fold and 31-fold increase in the bandpass filter response FSR. A microwave photonic bandpass filter with an even larger FSR can be realized by adjusting the second FS-ARDL loop length and by replacing the 750 MHz AOFS in the second loop with a SSB-SC modulator based frequency shifter that produces a larger frequency shift. A 40 GHz bandwidth SSB-SC modulator has been demonstrated [18] showing the large-FSR microwave photonic bandpass filter can be operated well into microwave frequencies. Note that the SSB-SC modulator is an electro-optic device and is implemented using lithium niobate technology. Hence, the FS-ARDL loop, which is formed by an optical coupler, an optical amplifier and a SSB-SC modulator based optical frequency shifter, can be fabricated on a lithium niobate waveguide [5], [6], [18]. This enables the large-FSR microwave photonic bandpass filter to be realized using two or more very small-delay high-frequency FS-ARDL modules.

5. Conclusion

The noise components in a new microwave photonic signal processing structure for realizing a large-FSR high-resolution bandpass filter response have been investigated. The filter is based on using the Vernier effect and the frequency shifting technique in an optical delay line structure. It solves, for the first time, both the limited FSR problem and the PIIN problem in the IIR-based optical delay line architectures. The power spectrum of the s-sp beat noise, which is the dominant noise source in the multiple FS-ARDL structure, has been analyzed and compared with the single FS-ARDL structure. Simulation results show the advantage of low-noise performance in the FS-ARDL remains in the dual-loop structure. Experimental results have been presented that demonstrate 31-fold increase in the FSR of a bandpass filter response. The results have also demonstrated a robust high-resolution bandpass filtering operation using a narrow-linewidth laser source. Furthermore, no PIIN was observed and high SNR performance was measured. The new photonic based filter offers bandpass filtering to microwave frequencies, which can be integrated in optical fiber microwave transmission systems.

References

[1] R. A. Minasian, "Photonic signal processing of microwave signals," *IEEE Trans. Microw. Theory Tech.*, vol. 54, no. 2, pp. 832–846, Feb. 2006.

[2] B. Moslehi and J. W. Goodman, "Novel amplified fiber-optic recirculating delay line processor," *J. Lightwave Technol.*, vol. 10, no. 8, pp. 1142–1146, Aug. 1992.

[3] E. H. W. Chan, K. E. Alameh, and R. A. Minasian, "Photonic bandpass filters with high skirt selectivity and stopband attenuation," *J. Lightwave Technol.*, vol. 20, no. 11, pp. 1962–1967, Nov. 2002.

[4] B. Vidal, V. Polo, J. L. Corral, and J. Marti, "Harmonic suppressed photonic microwave filter," *J. Lightwave Technol.*, vol. 21, no. 12, pp. 3150–3154, Dec. 2003.

[5] J. X. Chen, T. Kawanishi, K. Higuma, S. Shinada, J. Hodiak, M. Izutsu, W. C. Chang, and P. K. L. Yu, "Tunable lithium niobate waveguide loop," *IEEE Photon. Technol. Lett.*, vol. 16, no. 9, pp. 2090–2092, Sep. 2004.

[6] I. Baumann, S. Bosso, R. Brinkmann, R. Corsini, M. Dinand, A. Greiner, K. Schafer, J. Sochtig, W. Sohler, H. Suche, and R. Wessel, "Er-doped integrated optical devices in $LiNbO_3$," *IEEE J. Quantum Electron.*, vol. 2, no. 2, pp. 355–366, Jun. 1996.

[7] K. Oda, N. Takato, and H. Toba, "A wide-FSR waveguide double-ring resonator for optical FDM transmission systems," *J. Lightwave Technol.*, vol. 9, no. 6, pp. 728–736, Jun. 1991.

[8] K. Zhu, H. Ou, H. Fu, E. Remb, and S. He, "A simple and tunable single-bandpass microwave photonic filter of adjustable shape," *IEEE Photon. Technol. Lett.*, vol. 20, no. 23, pp. 1917–1919, Dec. 2008.

[9] L. Zhou, X. Zhang, E. Xu, Y. Yu, X. Li, and D. Huang, "A novel tunable cascaded IIR microwave photonic filter," *Opt. Commun.*, vol. 283, no. 14, pp. 2794–2797, Jul. 2010.

[10] E. Xu, X. Zhang, L. Zhou, Y. Zhang, Y. Yu, X. Li, and D. Huang, "Ultrahigh-Q microwave photonic filter with Vernier effect and wavelength conversion in a cascaded pair of active loops," *Opt. Lett.*, vol. 35, no. 8, pp. 1242–1244, Apr. 2010.

[11] B. Moslehi, "Analysis of optical phase noise in fiber-optic systems employing a laser source with arbitrary coherence time," *J. Lightwave Technol.*, vol. 4, no. 9, pp. 1334–1351, Sep. 1986.

[12] T. A. Nguyen, E. H. W. Chan, and R. A. Minasian, "A new technique for 100-fold increase in the FSR of optical recirculating delay line filters using a time compression unit," *Opt. Exp.*, vol. 20, no. 21, pp. 23 570–23 581, Oct. 2012.

[13] C. Pulikkaseril, E. H. W. Chan, and R. A. Minasian, "Coherence-free microwave photonic bandpass filter using a frequency-shifting recirculating delay line," *J. Lightwave Technol.*, vol. 28, no. 3, pp. 262–269, Feb. 2010.

[14] M. Asghari, I. H. White, and R. V. Penty, "Wavelength conversion using semiconductor optical amplifiers," *J. Lightwave Technol.*, vol. 15, no. 7, pp. 1181–1190, Jul. 1997.

[15] E. H. W. Chan, "High-order infinite impulse response microwave photonic filters," *J. Lightwave Technol.*, vol. 29, no. 12, pp. 1775–1782, Jun. 2011.

[16] M. R. Lee and S. Mecrow, "Noise characteristics of cascaded 2nd-order active filters," *Electron. Lett.*, vol. 12, no. 12, pp. 301–303, Jun. 1976.

[17] S. Shimotsu, S. Oikawa, T. Saitou, N. Mitsugi, K. Kubodera, T. Kawanishi, and M. Izutsu, "Single side-band modulation performance of a $LiNbO_3$ integrated modulator consisting of four-phase modulator waveguides," *IEEE Photon. Technol. Lett.*, vol. 13, no. 4, pp. 364–366, Apr. 2001.

[18] T. Kawanishi, T. Sakamoto, and M. Izutsu, "High-speed control of lightwave amplitude, phase and frequency by use of electro-optic effect," *IEEE J. Quantum Electron.*, vol. 13, no. 1, pp. 79–91, Jan./Feb. 2007.